Manuscript ID: DOEBTO-UMD-9158-21-TA1

Full Citation: Alam, T., Bacellar, D., Ling, J. and Aute, V. "**Numerical Study and Validation of Melting and Solidification in PCM Embedded Heat Exchangers with Straight Tube**." *18th International Refrigeration & Air Conditioning Conference*, Paper ID: 10079. May 24-28, 2021.

Numerical Study and Validation of Melting and Solidification in PCM Embedded Heat Exchangers with Straight Tube

Tanjebul Alam[1], Daniel Bacellar[1], Jiazhen Ling[1], Vikrant Aute[1]*
[1]University of Maryland, College Park, MD

*Corresponding Author

ABSTRACT

Latent heat thermal energy storage (LHTES) systems have shown great potential to enable reliable use of renewable energy and load shifting. LHTES offer high storage density and release energy at near constant temperature because of its use of phase change materials (PCMs). The cylindrical PCM heat exchangers (PCMHX) are one of the most used technologies due to their simplicity. Numerical models for such PCMHX enable engineers to estimate their performance for different design parameters and operating conditions without having to test them all. However, modeling the phase change phenomena can be challenging. To better understand the difficulties involving accurate modeling of PCMHX, a cylindrical latent storage unit filled with PCM and water as in-tube heat transfer fluid (HTF) is numerically investigated. This paper presents a study based on a 2D-axisymmetric model of a straight tube embedded in PCM in a cylindrical container. CFD is used to study the charging (melting) and discharging (solidification) phenomena. The models are validated against experimental and numerical data from the literature. The predicted local PCM temperature profile over time agrees within 2K compared to the experimental values. The paper also presents a simple method to estimate the melting and solidification phase change temperature range from limited data provided by PCM manufacturers.

Keywords: PCM, melting, solidification, CFD, heat exchanger

1. INTRODUCTION

One of the major obstacles to the widespread use of renewable power systems is their intermittent and unpredictable nature. It is essential to match the supply and demand of energy in different times of the day and often to store excess energy that would otherwise be wasted. To maintain uninterrupted power supply by limiting the fluctuation, implementation of energy storage system with renewable power systems is necessary. One of the forms of energy storage is the latent heat thermal energy storage (LHTES) system with phase change materials (PCMs). PCMs have high latent heat of fusion, and they absorb (melting) and release (solidification) energy in a narrow temperature range during phase transition between solid and liquid states.

Annular PCM storage is a common technique for storing latent energy and has been investigated extensively by researchers for both experimental and numerical studies. These devices are made up of two concentric cylinders where the heat transfer fluid (HTF) flows through the inner tube and the PCM fills up the annular space. Ismail and Abugderah (2000) and Trp et al. (2006) modeled these devices by removing the HTF, the tube wall domain and only taking diffusion as a heat transfer model in the PCM domain for simplification. While these studies provide simple numerical solution, they do not consider the effect of natural convection in the PCM domain. It has been experimentally shown by Ettouney et al. (2004), Agyenim et al. (2010) , Hosseini et al. (2012) and Longeon et al. (2013) that the natural convection plays a major role in the melting process of PCM. Numerical studies by Mesalhy et al. (2005), Longeon et al. (2013), Hosseini et al. (2014) and Pu et al. (2020) have discussed the necessity of considering natural convection for fitting the models with experimental results and their significant influence on the evolution of the PCM melting front.

Predicting the effect of natural convection in a model can be difficult as the natural convection depends on PCM thermophysical properties, thickness of molten PCM layer and the injection direction of HTF. One of the major difficulties to the modeling of PCMHX is the lack of information regarding thermophysical properties of PCMs. For instance, PCMs used in latent heat storage devices often have a temperature range for phase change and not a single melting or solidification point. Values for the phase-change temperature range along with viscosity and thermal expansion co-efficient for their products are rarely reported and so it is required to find a simple estimation method to determine these thermophysical properties of PCMs.

This paper presents a CFD based model for an annular PCMHX with straight tube which is experimentally and numerically validated with data from literature. This study also presents an estimation method of PCM melting and solidification temperature range based on the data available from manufacturers.

2. MODEL DESCRIPTION

2.1 Objectives and Subject of Study

Straight tube with PCMHX (Figure 1a) is a traditional heat exchanger geometry and the focus of this study is to develop numerical models which can predict the temperature profile of PCM in charging (melting) and discharging (solidification) processes and that can accurately estimate phase-change time. Longeon et al. (2013) presented a detailed experimental study of melting and solidification on a straight tube PCMHX which was used to validate our models. The geometry specification from this model is provided in Table 1. The geometry was modeled as a conventional full-sized axisymmetric domain (Figure 1b) - as it has been done extensively in the literature (e.g. (Pu et al., 2020) and (Zhang et al., 2020)).

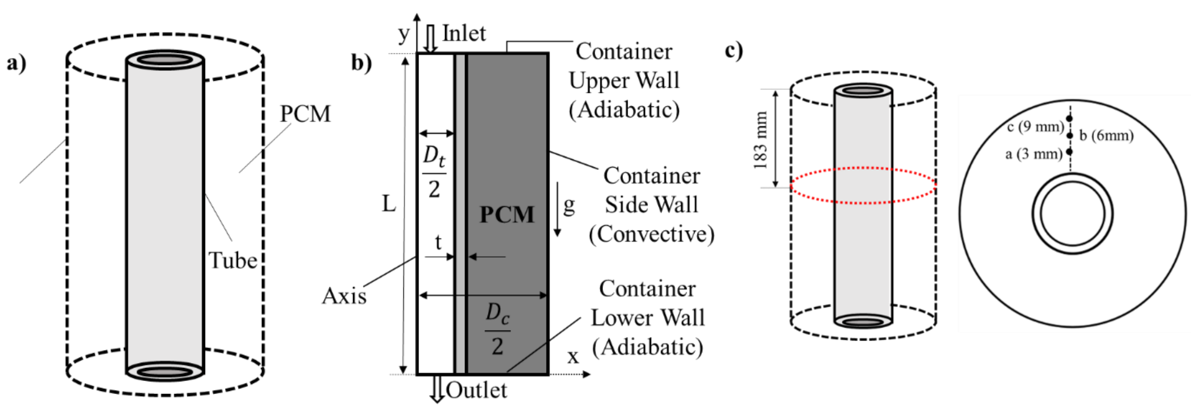

Figure 1: Schematic of a) Straight Tube PCM Embedded Heat Exchanger b) Computational Domain c) Thermocouple Positions

Table 1: Geometry Specifications

Dimension	**Unit**	**Value**
Tube Diameter - D_t	mm	15
Tube Wall Thickness - t	mm	2.5
Tube Length - L	mm	400
Tube Material	-	Stainless Steel
Container Diameter - D_c	mm	44

2.2 CFD Model

A complete 3D model including a conjugate heat transfer between working fluid and PCM illustrated in figure 1a, is computationally too intensive to solve in CFD. In the literature, this type of problem is often solved by employing axisymmetric conditions because of the axis symmetrical nature of the physical model (Figure 1b). In this work such a model was implemented in ANSYS Fluent 2019 R3. The HTF is water, flowing from top to bottom, at different temperatures for melting and solidification processes. Paraffin RT35 by Rubitherm GmbH (RUBITHERM GmbH, 2020) is used as the PCM.

The corresponding Reynolds number for the tube flow is 146 (Longeon et al., 2013) and hence a laminar flow model was used. The solidification and melting module in Fluent is used to simulate the phase-change process of PCM which uses the Enthalpy-porosity model (Voller & Prakash, 1987), (Voller et al., 1989). Natural convection is taken into consideration during PCM melting process using Boussinesq approximation. The uniform initial temperature conditions are 22 °C for melting and 40 °C for solidification. The initial velocity of the computation domain is zero. As seen from Figure 1b, the upper and lower container walls are modeled as thermal insulation and the left side of the container is used as an axis for the symmetry. Heat loss to ambient through container side wall is considered. An empirical correlation for natural convection is used to estimate the convective heat transfer coefficient between the container wall and the ambient (Pu et al., 2020). The estimated value of the heat transfer coefficient is 7.3 W/m^2-K. The ambient temperature is taken as 30°C based on the experiment (Longeon et al., 2013).

The settings for melting and solidification models are similar except the change in phase-change temperature range and water inlet temperature and PCM initial temperature. The structured rectangular grids are used to discretize the computational domain. A successful numerical melting model validation with the same experimental setup was found in literature (Pu et al., 2020) using a grid number size of 2.7×10^5 and a time step size of 0.1s. The same time and spatial discretization are used in this work. The PCM thermophysical properties, initial boundary conditions, and the general CFD settings used in this work are presented in Table 2.

Table 2: PCM Thermophysical Properties, Initial Boundary Conditions and CFD Settings

Property	Units	Method	Value(s)
Density	kg/m^3	Boussinesq	880
Specific Heat	kJ/kg-K	Piecewise Lin.	1.8(s)/ 2.4(l)
Thermal Conductivity	W/m-K	Constant	0.2
Viscosity	kg/m-s	Constant	0.0029
Thermal Expansion Coefficient	K^{-1}	Constant	0.001
Latent Heat	kJ/kg	Constant	157
Solidification Temperature Range	K	Constant	300.15-311.15
Melting Temperature Range	K	Constant	301.15-313.15
Initial Temperature -Melting	K	Constant	295.15
Water Inlet Temperature -Melting	K	Constant	325.15
Initial Temperature - Solidification	K	Constant	313.5
Water Inlet Temperature - Solidification	K	Constant	290.15
Ambient Temperature	K	Constant	303.15
Water Inlet Velocity	m/s	Constant	0.01

Settings	Value(s)
Pressure-Velocity Coupling	SIMPLE
Pressure Disc. Scheme	PRESTO!
Momentum Disc. Scheme	QUICK
Energy Discretization Scheme	QUICK
Continuity Conv. Criteria	10^{-5}
x-vel. Convergence Criteria	10^{-5}
y-vel. Convergence Criteria	10^{-5}
Energy Convergence Criteria	10^{-12}
Iterations per Time Step	40
Flow Regime Model	Laminar
Mushy Zone Parameter	10^6
Pressure Under Relaxation	0.3
Momentum Under Relaxation	0.7
Energy Under Relaxation	1

2.3 Estimation of Solidification and Melting Temperature Range

PCMs usually exhibit a temperature glide during the melting and solidification process instead of a constant temperature. The total enthalpy difference during this phase change comprises of sensible heat and the latent heat. The thermal behavior observed for PCMs within this temperature region is complex due to the flow of liquid PCM and hence, the accurate estimation of the temperature range is imperative for a reliable model. But temperature range values are not always available, so it is essential to develop an estimation method to determine the phase-change temperature range.

Latent heat of fusion/ solidification and partial enthalpy at different temperature points are one of the most featured PCM data reported by the manufacturers. This data is typically generated using a thermo-analytical technique called Differential Scanning Calorimetry (DSC). In DSC, the difference in the amount of heat required to increase the temperature of a sample and reference is measured as a function of temperature. DSC is widely used to detect phase-change; more or less heat will need to flow through it than the reference to maintain both at the same temperature.

However, the results from the DSC curve are greatly dependent on the sample size and the rate of heat flow through the PCM. (Longeon et al., 2013) showed in their study that the phase-change range shifts and flattens when the rate of heat flow increases. They suggested the use of a DSC curve in their study which has the same heat of fusion from the area below the curve but centered around the nominal melting temperature. This method can be used to select an optimum partial enthalpy curve based on the nominal melting temperature. After selecting the appropriate curve, the method proposed below can be used for estimating melting and solidification temperature ranges of different PCMs.

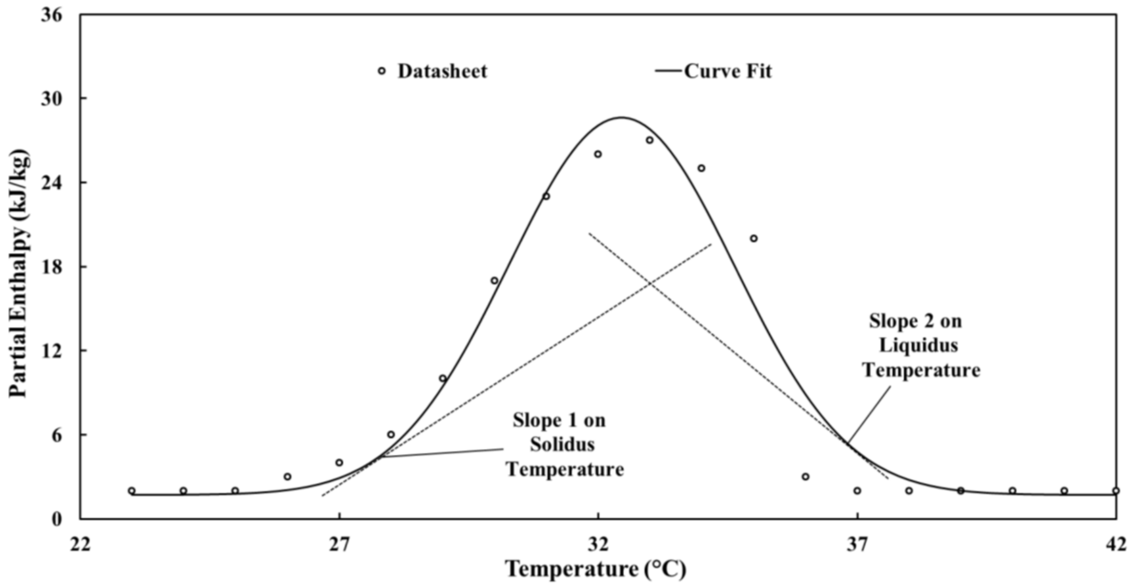

Figure 2: Using Partial Enthalpy Data for Melting and Solidification Range Estimation

Figure 2 shows the partial enthalpy data for a generic PCM and this data will be used to estimate the melting and solidification temperatures using the following method:

- Step 1 – Create a Gaussian curve fit from the partial enthalpy data.
- Step 2- The datasheet generally provides the latent heat for melting and solidification. Using the partial enthalpy data, it is possible to find out different combinations of temperature points for a high (liquidus) and a low (solidus) temperature. The difference of enthalpy in these points need to be close to the value of the latent heat of the PCM.
- Step 3- After getting different combinations of temperature points, it is possible to find the slopes on those points. Figure 2 shows the two slopes drawn on the high temperature and the low temperature. The high temperature indicates the melting point, and the low temperature indicates the solidification point. Comparing the slopes in different temperatures, it is possible to find out for which combination the value of the slopes is similar in high and low temperature. This combination will indicate the approximate solidus and liquidus temperatures.

Based on this method, for solidification the temperature range of 27 °C to 38 °C and for melting, 28 °C to 40 °C are found to be the most appropriate estimation. For the thermal expansion coefficient and the viscosity of RT35, we have used the value presented by (Pu et al., 2020). However, for different PCMs these values are not always reported, and they are generally determined using specific instruments (Delgado et al., 2018) which are not always widely accessible and can be an expensive process both in cost and time. To the best of our knowledge, there is no simple method to estimate these values for different PCMs. This is a significant gap in the research for the numerical modeling of PCMHX which needs more in-depth discussions, however, are beyond the scope of this work.

3. RESULTS

Figure 1c shows the scheme of the thermocouple positions inside the PCM container used in the reference experiment. (Longeon et al., 2013). We validate our model by placing virtual thermocouples in the same positions and comparing the temperature profiles.

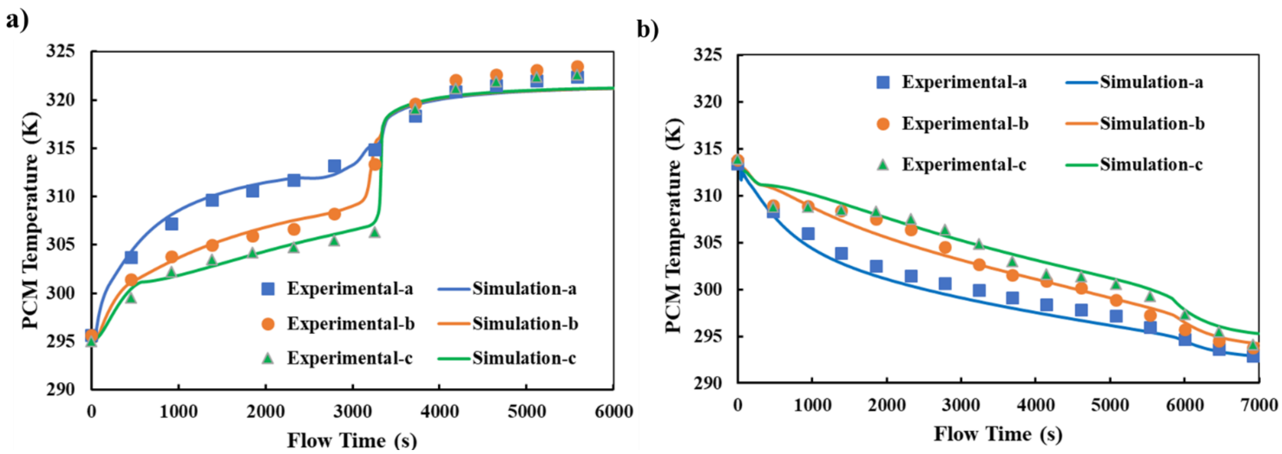

Figure 3: Comparison of Temperature Profile in a) Melting Model and b) Solidification Model with Experimental Results from Literature

Figure 3a shows the temperature profile during melting in the thermocouple positions mentioned above for the first 6000s flow time. This is compared with the experimental results from Longeon et al. (2013). It can be observed that the results of simulation agree well with the experimental results from literature. The deviation after 3000s can be attributed to the unknown angular position of the thermocouples and the overestimation of heat loss to the ambient. Figure 4a shows that the average liquid fraction of PCM compared to numerical results from Pu et al., (2020) for the same case.

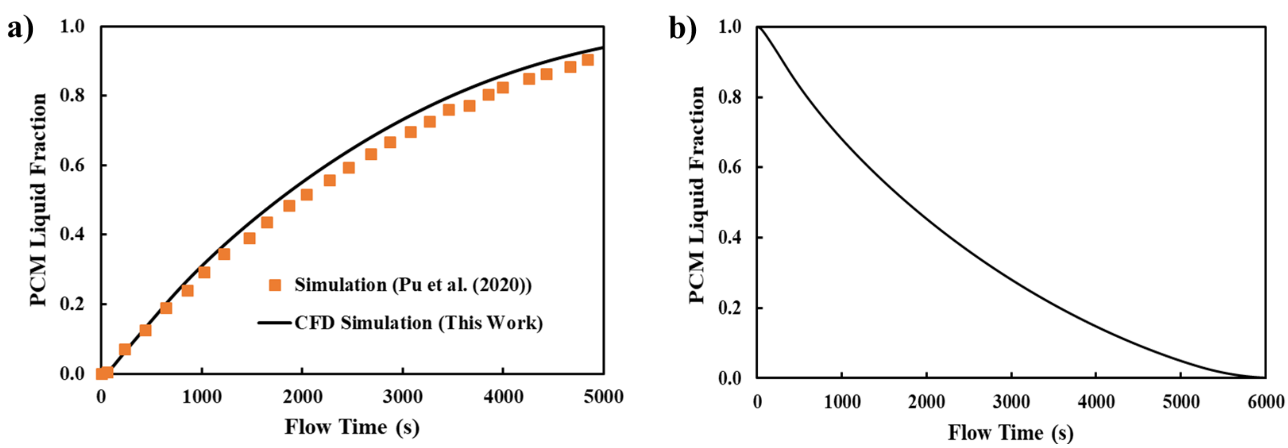

Figure 4: a) Comparison of Liquid Fraction in Melting Model with Numerical Results from Literature, b) Liquid Fraction in Solidification Model

Figure 3b shows the temperature profile during solidification for the thermocouple positions for the first 7000s. The thermocouple positions are same as the positions in melting model. This is compared with the experimental results from Longeon et al. (2013). It is evident that the results are in very good agreement with the experimental data. The predicted PCM temperature profile in both the models agrees well within 2K over time compared to the experimental data. Figure 4b shows the average liquid fraction over time for the solidification model.

Figure 5a and 5b shows the comparison of experimental and predicted outlet temperature of water in models for melting and solidification respectively. The prediction of outlet water temperature matches very closely in solidification process compared to the melting process. In the melting process the deviation from experimental outlet temperature increases over time. This can be attributed to overestimation of heat loss to the ambient. With time, the temperature of PCM increases in the model and this increases the amount of heat loss. Compared to the melting model, the temperature difference in PCM and ambient was lower in solidification process which results in lower heat loss.

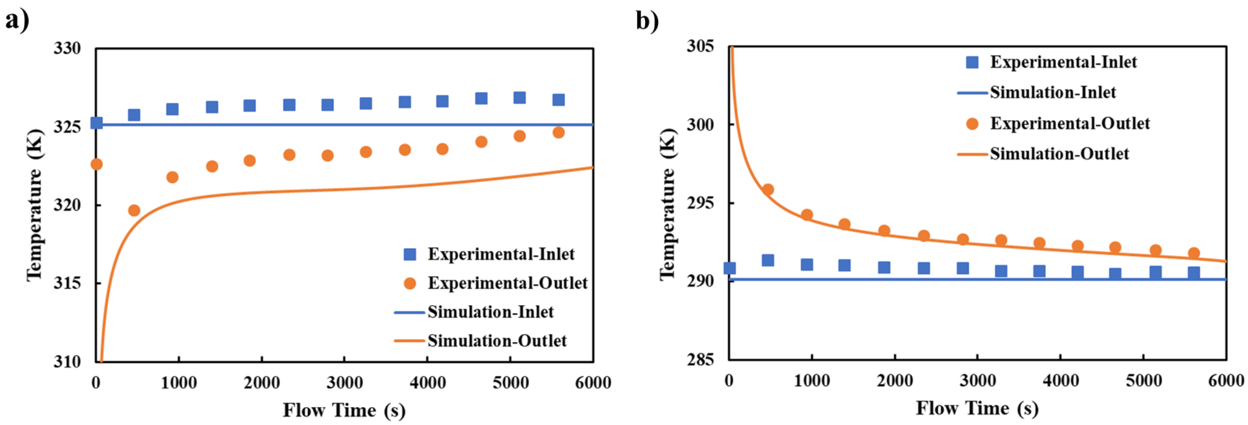

Figure 5: Comparison of Experimental and Numerical Water Inlet and Outlet Temperature for a) Melting b) Solidification

Figure 6a and 6b shows the comparison of experimental and numerical heat flow rate of water for melting and solidification process respectively. The experimental heat flow rate was calculated assuming a constant flow rate based on the average velocity from Longeon et al. (2013). The deviation of heat flow from the experiments is higher in the melting model because of higher deviation in outlet temperature prediction as shown in Figure 5a. But overall, both the models show similar trend in heat flow rate when compared to the experimental results.

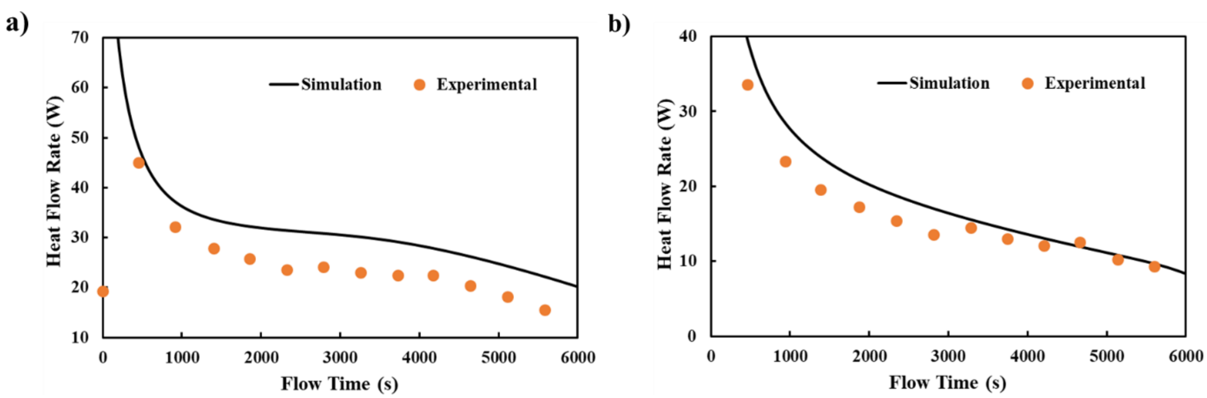

Figure 6: Comparison of Experimental and Numerical Water Heat Flow Rate for a) Melting, b) Solidification

Table 3 summarizes the hardware information and the computational cost. The solidification model took approximately half the time to simulate first 6000s of flow time compared to the melting model. During the solidification, the mode of heat transfer from the tube wall to PCM is mainly conduction as the PCM near the tube wall solidifies first. With time, PCM around the container begins to solidify and amount of molten PCM reduces. In case of melting, the heat transfer from the tube wall to the PCM is a combination of both conduction and natural convection due to the motion of liquid PCM near the tube wall.

Table 3: Hardware Information and Computational Cost

Hardware

No. of Cores	Processor	RAM (Gigabyte)
28	2 x Intel® Xeon® Gold 5117, 2.00 GHz	96
Computational Cost		
Model	**Simulated time (s)**	**Computation Time (hour)**
Melting	6000 (Full)	105
Solidification	6000 (First)	50
	7000 (Full)	56

4. CONCLUSIONS

Numerical models for melting and solidification in a straight tube PCMHX have been developed and validated against numerical and experimental data from literature. A simple method to estimate the melting and solidification phase-change temperature ranges was also presented. The models took approximately 105 hours and 50 hours to simulate 6000s of flow time for melting and solidification respectively. The melting model may have taken longer time because it takes more time to solve the combined effect of conduction and natural convection. The validation shows that the predicted PCM temperature profile over time agrees within 2K compared to the experimental values. Future work includes investigating removal of in-tube flow and replacing with convective or constant wall boundary conditions to improve the computational time while maintaining accuracy.

NOMENCLATURE

D_c	Container Diameter	(mm)
D_t	Tube Diameter	(mm)
L	Length	(mm)
T_s	Solidus Temperature	(°C)
T_l	Liquidus Temperature	(°C)
t	Tube Wall Thickness	(mm)

REFERENCES

Agyenim, F., Eames, P., & Smyth, M. (2010). Heat transfer enhancement in medium temperature thermal energy storage system using a multitube heat transfer array. *Renewable Energy*, *35*(1), 198–207. https://doi.org/10.1016/j.renene.2009.03.010

Delgado, M., Lázaro, A., Biedenbach, M., Gamisch, S., Gschwander, S., Höhlein, S., … Brüggemann, D. (2018). Intercomparative tests on viscosity measurements of phase change materials. *Thermochimica Acta*, *668*, 159–168. https://doi.org/https://doi.org/10.1016/j.tca.2018.08.017

Ettouney, H. M., Alatiqi, I., Al-Sahali, M., & Ahmad Al-Ali, S. (2004). Heat transfer enhancement by metal screens and metal spheres in phase change energy storage systems. *Renewable Energy*, *29*(6), 841–860. https://doi.org/https://doi.org/10.1016/j.renene.2003.11.003

Hosseini, M. J., Rahimi, M., & Bahrampoury, R. (2014). Experimental and computational evolution of a shell and tube heat exchanger as a PCM thermal storage system. *International Communications in Heat and Mass Transfer*, *50*, 128–136. https://doi.org/10.1016/j.icheatmasstransfer.2013.11.008

Hosseini, M. J., Ranjbar, A. A., Sedighi, K., & Rahimi, M. (2012). A combined experimental and computational study on the melting behavior of a medium temperature phase change storage material inside shell and tube heat exchanger. *International Communications in Heat and Mass Transfer*, *39*(9), 1416–1424. https://doi.org/10.1016/j.icheatmasstransfer.2012.07.028

Ismail, K. A. R., & Abugderah, M. M. (2000). Performance of a thermal storage system of the vertical tube type. *Energy Conversion and Management*, *41*(11), 1165–1190. https://doi.org/10.1016/S0196-8904(99)00140-5

Longeon, M., Soupart, A., Fourmigué, J. F., Bruch, A., & Marty, P. (2013). Experimental and numerical study of annular PCM storage in the presence of natural convection. *Applied Energy*, *112*, 175–184. https://doi.org/10.1016/j.apenergy.2013.06.007

Mesalhy, O., Lafdi, K., Elgafy, A., & Bowman, K. (2005). Numerical study for enhancing the thermal conductivity of phase change material (PCM) storage using high thermal conductivity porous matrix. *Energy Conversion and Management*, *46*(6), 847–867. https://doi.org/https://doi.org/10.1016/j.enconman.2004.06.010

Pu, L., Zhang, S., Xu, L., & Li, Y. (2020). Thermal performance optimization and evaluation of a radial finned shell-and-tube latent heat thermal energy storage unit. *Applied Thermal Engineering*, *166*(November 2019), 114753. https://doi.org/10.1016/j.applthermaleng.2019.114753

RUBITHERM GmbH. (2020). RUBITHERM RT 35 Phase change material. Retrieved from https://www.rubitherm.eu/media/products/datasheets/Techdata_-RT35_EN_09102020.PDF

Trp, A., Lenic, K., & Frankovic, B. (2006). Analysis of the influence of operating conditions and geometric parameters on heat transfer in water-paraffin shell-and-tube latent thermal energy storage unit. *Applied Thermal Engineering*, *26*(16), 1830–1839. https://doi.org/10.1016/j.applthermaleng.2006.02.004

Voller, V. R., Brent, A. D., & Prakash, C. (1989). The modelling of heat, mass and solute transport in solidification systems. *International Journal of Heat and Mass Transfer*, *32*(9), 1719–1731. https://doi.org/https://doi.org/10.1016/0017-9310(89)90054-9

Voller, V. R., & Prakash, C. (1987). A fixed grid numerical modelling methodology for convection-diffusion mushy region phase-change problems. *International Journal of Heat and Mass Transfer*, *30*(8), 1709–1719. https://doi.org/10.1016/0017-9310(87)90317-6

Zhang, S., Pu, L., Xu, L., Liu, R., & Li, Y. (2020). Melting performance analysis of phase change materials in different finned thermal energy storage. *Applied Thermal Engineering*, *176*(March), 115425. https://doi.org/10.1016/j.applthermaleng.2020.115425

ACKNOWLEDGEMENTS

This material is based upon work supported by the U.S. Department of Energy's Office of Energy Efficiency and Renewable Energy (EERE) under the Building Technologies Office Award Number DE-EE0009158. The views expressed herein do not necessarily represent the views of the U.S. Department of Energy or the United States Government. This work was also funded in part by the Modeling and Optimization Consortium at the University of Maryland.